Antiphase dynamics and self-pulsing due to a low-frequency spatial population grating in a multimode laser

G. Kozyreff and Paul Mandel
Optique Nonlinéaire Théorique, Université Libre de Bruxelles, Campus Plaine Code Postal 231, B-1050 Bruxelles, Belgium
(Received 7 April 1998)

We study analytically equations that extend the Tang-Statz-deMars rate equations for a multimode Fabry-Perot laser by including the low-spatial-frequency population grating and the inhomogeneous pumping rate along the cavity axis [Quant. Semiclassic Opt. **5**, L17 (1997)]. First, we prove the theorem that is the foundation of the antiphase dynamics: The total intensity transients are characterized by only one frequency, the single-mode relaxation oscillation. Second, we study the three-mode laser operation. In this context, we derive analytic expressions for the steady-state intensities, their linear stability, and the bifurcation points. We prove that strictly multimode solutions display a Hopf bifurcation leading to passive *Q*-switched solutions. Numerically, we have found that these time-periodic regimes may bifurcate to quasiperiodic and chaotic states and that there are many domains of bistability. [S1050-2947(98)07012-7]

PACS number(s): 42.65.Sf, 42.55.Rz, 42.60.Rn

I. INTRODUCTION

The problem of an adequate description of a multimode homogeneously broadened Fabry-Perot laser in the rate equation limit is old. By rate equations we mean equations that couple the fields and the population inversion. A successful model was proposed by Tang, Statz, and deMars [1], who showed that the dominant feature driving these lasers was the coupling between the modal intensities and the average population inversion via the population inversion grating (also known as spatial hole burning) at optical wavelengths. Soon afterward, a number of theoretical models generalizing the Tang-Statz-deMars (TSD) equations were proposed to account for additional mechanisms: the coupling among the complex field modal amplitudes (phase-sensitive interactions), the coupling between the complex field modal amplitudes and the population grating at either optical or/and long wavelengths, and the longitudinal inhomogeneity of the pumping mechanism [2–8]. The TSD^+ model [9] is a recent extension of the TSD model that includes (i) the coupling of the modal intensities to the low spatial frequencies of the inversion of population profile and (ii) the pump profile in the longitudinal direction. Transverse effects are ignored in this approach. This paper is devoted to a systematic study of the TSD^+ model. It is justified by some recent unpublished results, which suggest that microchip lasers may be better described by the TSD^+ rate equations than by the traditional TSD equations.

In Sec. II we briefly recall the two rate equation models and define the notation. In Sec. III we prove that a fundamental theorem of antiphase dynamics, which was demonstrated for the TSD equations, is preserved by the TSD^+ extension. This theorem deals with the properties of the total intensity, which in the rate equation approximation is the sum of the modal intensities. It states that in the limit of a flat gain curve, the deviation of the steady state of the total intensity is a global variable verifying a single linear harmonic oscillator equation with a frequency Ω_R that is mode independent. This relaxation oscillation frequency generates a peak in the power spectrum of the total intensity when the laser is subjected to an external perturbation (noise, weak modulation, and transient relaxation, for instance). This is in contrast with the modal intensities that display a larger number of peaks, typically as many peaks (and therefore relaxation oscillation frequencies) as there are modes, and possibly the harmonics of these frequencies.

In Sec. IV we analyze systematically a symmetric three-mode configuration with one central mode of maximum gain $\gamma_{\max}$ and two side modes with equal gains smaller than or equal to $\gamma_{\max}$. There are two types of steady solutions: regular and marginal solutions. By regular we mean a solution that is defined in a finite domain of the three-dimensional (3D) parameter space of the pumping rates. The marginal solutions exist only on hypersurfaces of this 3D space and are therefore expected to be much more difficult to observe. The necessity to consider these marginal solutions stems from the fact that they are necessary to connect the regular solutions. However, since there are large domains of multistability, it may very well be that the marginal solutions are not observed in an experiment and that a jump transition to another regular state occurs. For the regular solutions, we give the expressions of the steady-state solution and determine their stability. For the marginal solutions, we only give an expression of their steady state. In particular, in Sec. IV E we analyze the Hopf bifurcations that may destabilize multimode solutions only. Given the difficulty to determine the existence and stability character of these bifurcations in the usual way (i.e., nonlinear stability analysis of the steady state), we adopt an alternative approach, which is suggested by the numerical simulations of the TSD^+ equations. Indeed, they are prone to display pulsed solutions, as in a passive *Q*-switching process. On this basis, we assume the existence of pulsed solutions and determine analytically the conditions of existence of an interpulse solution, in which the modal intensities are vanishingly small. It turns out that this problem can be solved analytically and the conditions of existence are identical to the Hopf bifurcation conditions whenever a straightforward analysis has been possible. In

addition, this result suggests that the Hopf bifurcations of the steady states are subcritical.

II. THE TSD$^+$ MODEL

Let us consider a cavity lasing on $\mathcal{N}$ successive longitudinal modes of the cavity with frequencies ν_n between $m_0 c/2L$ and $(m_0+\mathcal{N}-1)c/2L$, L being the length of the cavity. The usual TSD model yields the $2\mathcal{N}+1$ equations

$$\frac{dD_0}{dt} = w_0 - \left(1+\sum_m \gamma_m I_m\right) D_0 + \sum_m \gamma_m I_m N_m,$$

$$\frac{dN_n}{dt} = -\left(1+\sum_m \gamma_m I_m\right) N_n + \frac{1}{2}\gamma_n I_n D_0,$$

$$\frac{dI_n}{dt} = kI_n[-1+\gamma_n(D_0-N_n)] \quad \text{with} \quad n,m=1,\ldots,\mathcal{N}.$$

The time t is expressed in units of the population inversion characteristic time of relaxation $\gamma_\parallel^{-1}$. The constant k is the inverse of the photon lifetime inside the cavity in the same units. The population inversion is expanded according to

$$D(z,t) = C\sum_{n=0}^{\mathcal{N}} D_n \cos\left(\frac{2n\pi z}{L}\right) + C\sum_{n=1}^{\mathcal{N}} N_n \cos\left(\frac{2(m_0+n-1)\pi z}{L}\right),$$

where C is chosen so that $D_0=1$ is the lasing first threshold. Note that $m_0 \sim 10^6$, so that the $\{N_n\}$ describes the population grating at the optical wavelength while $\{D_n\}$ describes the population grating at long wavelengths, which correspond to the beat notes between lasing modes. The pumping $w(z)$ is projected on the long-wavelength cavity modes

$$w(z) = \sum_{n=0}^{\mathcal{N}} w_n \cos\left(\frac{2n\pi z}{L}\right).$$

The frequency detuning of mode n from atomic resonance is $\Delta_n = (\nu_n - \omega_{at})/\gamma_\perp$. The normalized gain parameters are

$$\gamma_n = \frac{1+\Delta_*^2}{1+\Delta_n^2}, \quad n=1,\ldots,\mathcal{N},$$

where $\Delta_* = \min_n \Delta_n$.

The TSD model only couples w_0, D_0, and the $\{N_n\}$ to the modal intensities I_n. On the contrary, the TSD$^+$ model [9] yields the set of $3\mathcal{N}$ equations

$$\frac{dD_q}{dt} = w_q - \left(1+\sum_{m=1}^{\mathcal{N}} \gamma_m I_m\right) D_q + \frac{1}{2}\sum_{m=1}^{\mathcal{N}-q} \gamma_m I_m N_{m+q} + \frac{1}{2}\sum_{m=1+q}^{\mathcal{N}} \gamma_m I_m N_{m-q}, \quad (1)$$

$$\frac{dN_n}{dt} = -\left(1+\sum_{m=1}^{\mathcal{N}} \gamma_m I_m\right) N_n + \frac{1}{2}\sum_{m=1}^{\mathcal{N}} \gamma_m I_m D_{n-m}, \quad (2)$$

$$\frac{dI_n}{dt} = kI_n[-1+\gamma_n(D_0-N_n)], \quad n=1,\ldots,\mathcal{N}$$

$$q=0,\ldots,\mathcal{N}-1. \quad (3)$$

They describe the influence of the low spatial frequency population grating $\{D_q; q\neq 0\}$ on the laser dynamics.

III. ANTIPHASE DYNAMICS: A THEOREM

In this section we use an asymptotic expansion of the TSD$^+$ equations to prove that a fundamental theorem of antiphase dynamics, which was derived for the TSD equations, also holds for the TSD$^+$ equations. Let $\mathcal{Q}$ be the set of indices of the excited modes in the cavity $\mathcal{Q}=\{q|\overline{I}_q\neq 0\}$. Let $(\overline{I}_q,\overline{D}_q,\overline{N}_q)$ be the stationary values of (I_q,D_q,N_q). We introduce a small parameter $\varepsilon = 1/\sqrt{k}$ since k is typically a large parameter in the range 10^4–10^6. Following [10], we introduce a perturbation expansion around the steady state

$$D_q(t) = \overline{D}_q + \varepsilon^2 d_q(t) + O(\varepsilon^3),$$

$$N_n(t) = \overline{N}_n + \varepsilon^2 n_n(t) + O(\varepsilon^3),$$

$$I_n(t) = \overline{I}_n + \varepsilon i_n(t) + O(\varepsilon^2), \quad q=1,\ldots,\mathcal{N}, \quad n\in\mathcal{Q}.$$

We also use the time scale $\tau = t/\varepsilon$ because it is closely related to the relaxation frequencies of the system that are of the order of $\sqrt{k}$ as discussed in [11,12]. Moreover, it is assumed that the gain parameters are close to each other. This means that the gain curve is flat over the frequency spread of the lasing modes. Hence the gains are expanded as $\gamma_n = 1 - \varepsilon g_n + O(\varepsilon^2)$. To dominant order in ε, we obtain

$$\frac{dd_q}{d\tau} = -\overline{D}_q \sum_{m\in\mathcal{Q}} i_m + \frac{1}{2}\sum_{m=1,m\in\mathcal{Q}}^{\mathcal{N}-q} i_m \overline{N}_{m+q} + \frac{1}{2}\sum_{m=1+q,m\in\mathcal{Q}}^{\mathcal{N}} i_m \overline{N}_{m-q}, \quad (4)$$

$$\frac{dn_n}{d\tau} = -\overline{N}_n \sum_{m\in\mathcal{Q}} i_m + \frac{1}{2}\sum_{m\in\mathcal{Q}} i_m \overline{D}_{n-m}, \quad (5)$$

$$\frac{di_n}{d\tau} = \overline{I}_n(d_0-n_n) \quad \forall \ n\in\mathcal{Q}. \quad (6)$$

Note that for the excited modes, stationarity implies

$$\overline{N}_n = \overline{D}_0 - \frac{1}{\gamma_n} = \overline{D}_0 - 1 + O(\varepsilon). \quad (7)$$

This leads to

$$\frac{dd_0}{d\tau} = -\sum_{m\in\mathcal{Q}} i_m, \quad (8)$$

which explains the peculiar ε expansion used for the intensities.

We now study the evolution of the total intensity $I_T = \Sigma_{m\in\mathcal{Q}} I_m = \Sigma_{m\in\mathcal{Q}} \overline{I}_m + \Sigma_{m\in\mathcal{Q}} i_m$. We sum the linearized

equations (6) over $n \in \mathcal{Q}$ and derive the sum with respect to τ, taking Eqs. (5) and (8) into account, to obtain

$$\begin{aligned}\frac{d^2}{d\tau^2}\sum_{n\in\mathcal{Q}} i_n &= -\sum_{m\in\mathcal{Q}} i_m \sum_{n\in\mathcal{Q}} \overline{I}_n - \sum_{n\in\mathcal{Q}} \overline{I}_n \frac{dn_n}{d\tau} \\ &= -\sum_{m\in\mathcal{Q}} i_m \sum_{n\in\mathcal{Q}} \overline{I}_n + \sum_{n\in\mathcal{Q}} \overline{I}_n \overline{N}_n \sum_{m\in\mathcal{Q}} i_m \\ &\quad - \frac{1}{2}\sum_{n\in\mathcal{Q}} \overline{I}_n \sum_{m\in\mathcal{Q}} i_m \overline{D}_{n-m} \\ &= -\sum_{m\in\mathcal{Q}} i_m \sum_{n\in\mathcal{Q}} [\overline{I}_n(1-\overline{N}_n)] \\ &\quad - \frac{1}{2}\sum_{m\in\mathcal{Q}} i_m \sum_{n\in\mathcal{Q}} \overline{I}_n \overline{D}_{n-m}. \end{aligned} \tag{9}$$

Let us prove the lemma that $\Sigma_{n\in\mathcal{Q}}\overline{I}_n\overline{D}_{n-m}$ is independent of $m \in \mathcal{Q}$. It follows from Eq. (2) that

$$0 = -\left(1 + \sum_{m=1}^{\mathcal{N}} \gamma_m \overline{I}_m\right)\overline{N}_n + \frac{1}{2}\sum_{m=1}^{\mathcal{N}} \gamma_m \overline{I}_m \overline{D}_{n-m}.$$

To dominant order in ε, $\gamma_n = 1$, and $\overline{N}_n = \overline{D}_0 - 1$ for $n \in \mathcal{Q}$. In addition, $\overline{D}_p \equiv \overline{D}_{-p}$ by definition and we can replace $\Sigma_{m=1}^{\mathcal{N}}\overline{I}_m\overline{D}_{n-m}$ by $\Sigma_{m=1}^{\mathcal{N}}\overline{I}_m\overline{D}_{m-n}$. Then

$$\begin{aligned}\frac{1}{2}\sum_{m\in\mathcal{Q}} \overline{I}_m\overline{D}_{m-n} &= \left(1 + \sum_{m\in\mathcal{Q}} \overline{I}_m\right)\overline{N}_n \\ &= \left(1 + \sum_{m\in\mathcal{Q}} \overline{I}_m\right)(\overline{D}_0 - 1),\end{aligned}$$

which is the required lemma. Equation (1) for $q = 0$ and in a steady state yields $w_0 = \overline{D}_0 + \Sigma_{n\in\mathcal{Q}}\overline{I}_n$. Introducing this result in Eq. (9) and using Eq. (7) leads to

$$\left(\frac{d^2}{d\tau^2} + w_0 - 1\right)\sum_{n\in\mathcal{Q}} i_n = 0,$$

which is the theorem we wanted to prove: Deviations from the total steady-state intensity oscillate with only one frequency, the single mode relaxation oscillation frequency, no matter how many modes are lasing in the cavity. The dimensionless oscillation frequency is $\sqrt{w_0 - 1}$ or, equivalently, $\sqrt{(w_0-1)/\tau_c\tau_f}$ in s^{-1}, where τ_f and τ_c are, respectively, the fluorescence lifetime (i.e., the population inversion lifetime) and the cavity photon lifetime. This frequency is often referred to as the McCumber frequency and denoted Ω_R.

IV. STUDY OF A THREE-MODE REGIME

In this section we study the properties of the TSD$^+$ equations for a special case of the three-mode oscillation. The mode with the highest gain is labeled 1. Modes 2 and 3 are assumed to have the same gain parameter $\gamma \leqslant 1$. Thus the optical frequencies ν_j of modes j are connected by the relations $\nu_2 = \nu_1 - c/2L$ and $\nu_3 = \nu_1 + c/2L$. The pump distribution is

$$w(z) = w_0 + w_1\cos(2\pi z/L) + w_2\cos(4\pi z/L). \tag{10}$$

The stationary states are characterized by the nonzero modal intensities $\mathcal{R}$. We will therefore use this set to refer to the different steady states. For instance, the three possible monomode states will be denoted $\mathcal{R}_k = \{I_k\}$. The TSD$^+$ equations for this symmetric three-mode configuration that we study are

$$\frac{dD_0}{dt} = w_0 - (1 + \gamma I_2 + I_1 + \gamma I_3)D_0 + (\gamma I_2 N_2 + I_1 N_1 + \gamma I_3 N_3), \tag{11}$$

$$\frac{dD_1}{dt} = w_1 - (1 + \gamma I_2 + I_1 + \gamma I_3)D_1 + \frac{1}{2}(\gamma I_2 N_1 + I_1 N_2 + I_1 N_3 + \gamma I_3 N_1), \tag{12}$$

$$\frac{dD_2}{dt} = w_2 - (1 + \gamma I_2 + I_1 + \gamma I_3)D_2 + \frac{1}{2}(\gamma I_2 N_3 + \gamma I_3 N_2), \tag{13}$$

$$\frac{dN_1}{dt} = -(1 + \gamma I_2 + I_1 + \gamma I_3)N_1 + \frac{1}{2}(\gamma I_2 D_1 + I_1 D_0 + \gamma I_3 D_1), \tag{14}$$

$$\frac{dN_2}{dt} = -(1 + \gamma I_2 + I_1 + \gamma I_3)N_2 + \frac{1}{2}(\gamma I_2 D_0 + I_1 D_1 + \gamma I_3 D_2), \tag{15}$$

$$\frac{dN_3}{dt} = -(1 + \gamma I_2 + I_1 + \gamma I_3)N_3 + \frac{1}{2}(\gamma I_2 D_2 + I_1 D_1 + \gamma I_3 D_0), \tag{16}$$

$$\frac{dI_1}{dt} = k[-1 + (D_0 - N_1)]I_1, \tag{17}$$

$$\frac{dI_2}{dt} = k[-1 + \gamma(D_0 - N_2)]I_2, \tag{18}$$

$$\frac{dI_3}{dt} = k[-1 + \gamma(D_0 - N_3)]I_3. \tag{19}$$

In the three-mode configuration with $\gamma_1 = 1$, $\gamma_2 = \gamma_3 = \gamma < 1$, the TSD model predicts via a linear stability analysis

TABLE I. Modal selection as a function of the pump profile $w(z)=w_0+w_1\cos(2\pi z/L)+w_2\cos(4\pi z/L)$. The frequencies of modes 2 and 3 are $\nu_2=\nu_1-c/2L$ and $\nu_3=\nu_1+c/2L$, respectively.

Pump profile components	Maximum pump profile	Minimum pump profile	Favored pairs	Quenched pairs
$w_1>0$	$z=0,L$	$z=L/2$		$(I_1,I_2),(I_1,I_3)$
$w_1<0$	$z=L/2$	$z=0,L$	$(I_1,I_2),(I_1,I_3)$	
$w_2>0$	$z=0,L/2,L$	$z=L/4,3L/4$	$(I_1,I_2),(I_1,I_3)$	(I_2,I_3)
$w_2<0$	$z=L/4,3L/4$	$z=0,L/2,L$	(I_2,I_3)	$(I_1,I_2),(I_1,I_3)$

that only three stable constant solutions can exist: the trivial solution $\{\varnothing\}$, one monomode solution $\{\overline{I_1}\}$, and the three-mode solution $\{\overline{I_1},\overline{I_2},\overline{I_3}\}$.

For $w_0<1$, all intensities vanish. As w_0 is increased beyond the laser first threshold $w_{0,1}=1$, the laser enters the monomode regime until a second threshold $w_{0,2}=\gamma^{-1}$ is reached where $\overline{I_2}$ and $\overline{I_3}$ become simultaneously positive. In addition, the only stable solutions are constant in time.

Let us now analyze the TSD$^+$ equations (11)–(19). It is often simpler to express steady-state solutions and stability conditions in terms of the triplet $(\overline{D_0},\overline{D_1},\overline{D_2})$ than in terms of (w_0,w_1,w_2). The inversion of the relations $w_i=f_i(\overline{D_0},\overline{D_1},\overline{D_2})$, $i=0,1,2$, leads to complicated expressions that obscure the physical interpretation. However, $\overline{D_k}\to w_k$ in the absence of light-matter interaction. As a consequence, the stability conditions expressed with the $\overline{D_k}$ give a qualitative indication of the constraints imposed on w_k.

From Eqs. (17)–(19) a stable zero modal intensity, say $\overline{I_q}=0$, requires $-1+\gamma_q(\overline{D_0}-\overline{N_q})<0$. We infer the stability condition

$$\overline{N_q}(\overline{D_0},\overline{D_1},\overline{D_2})>\overline{D_0}-\gamma_q^{-1}. \tag{20}$$

Note that this is only a necessary condition. At the boundary $\overline{N_q}(\overline{D_0},\overline{D_1},\overline{D_2})=\overline{D_0}-\gamma_q^{-1}$, the system undergoes the stationary bifurcation $\mathcal{R}\to\mathcal{R}'=\mathcal{R}\cup\{\overline{I_q}\}$.

A key feature of the present analysis is that there are regions inside the cavity where longitudinal intensity distributions almost do not overlap for pairs of modes. Through spatial hole burning, one can expect more (less) efficient electric field amplification with increased (decreased) pump intensity in these regions when such pairs are excited. As a consequence, a nonuniform pumping distribution alters the mode competition. This is realized by tuning the pump parameters w_k in Eq. (10). A minimal overlap between longitudinal cavity eigenmodes is found at $z=L/2$ for the pairs $(\overline{I_1},\overline{I_2})$ and $(\overline{I_1},\overline{I_3})$ and at $z=L/2\pm L/4$ for the pair $(\overline{I_2},\overline{I_3})$. The role of w_1 and w_2 is therefore to distribute the injected energy among the modes of the cavity. A classification of the possible situations is given in Table I.

The steady-state solutions can be classified as follows: the trivial solution $\{\varnothing\}$, $\overline{I_1}=\overline{I_2}=\overline{I_3}=0$; the single-mode solutions $\{\overline{I_k}\}$, $\overline{I_k}>0$, $\overline{I_{j\neq k}}=0$; the two-mode solutions $\{\overline{I_1},\overline{I_2}\}$, $\overline{I_1}>0$, $\overline{I_2}\neq\overline{I_1}>0$, $\overline{I_3}=0$; $\{\overline{I_2},\overline{I_3}\}$, $\overline{I_1}=0$, $\overline{I_2}=\overline{I_3}>0$; and $\{\overline{I_2},\overline{I_3}\}^*$, $\overline{I_1}=0$, $\overline{I_2}\neq\overline{I_3}>0$; the three-mode solutions $\{\overline{I_1},\overline{I_2},\overline{I_3}\}$, $\overline{I_1}>0$, $\overline{I_2}=\overline{I_3}>0$; $\{\overline{I_1},\overline{I_2},\overline{I_3}\}^*$, $\overline{I_1}>0$, $\overline{I_2}\neq\overline{I_3}>0$, $\lim_{\gamma\to1}\overline{I_1}\neq\lim_{\gamma\to1}(\overline{I_2}+\overline{I_3})$; and $\{\overline{I_1},\overline{I_2},\overline{I_3}\}^{**}$, $\overline{I_1}>0$, $\overline{I_2}\neq\overline{I_3}>0$, $\lim_{\gamma\to1}\overline{I_1}=\lim_{\gamma\to1}(\overline{I_2}+\overline{I_3})$.

The solutions $\{\overline{I_2},\overline{I_3}\}^*$, $\{\overline{I_1},\overline{I_2},\overline{I_3}\}^*$, and $\{\overline{I_1},\overline{I_2},\overline{I_3}\}^{**}$ are necessary to provide a connection between the other solutions. However, they exist only along lines or surfaces in the 3D pump parameter space and therefore are of measure zero.

A. Trivial solution $\{\varnothing\}$

The trivial solution is

$$\overline{I_k}=\overline{N_k}=0,\quad \overline{D_l}=w_l,\quad k=1,2,3,\quad l=0,1,2.$$

The stability of the trivial solution is ruled by the root $\lambda=k(\overline{D_0}-1)$. The trivial solution is stable if $w_0<1$. At $w_0=1$, a steady bifurcation leads to the monomode solution $\{\overline{I_1}\}$.

In addition, there are bifurcations from the unstable section of the $\{\varnothing\}$ solution to solutions that emerge as unstable states. We list them because such solutions may become stable. For γ arbitrary, the solutions $\{\overline{I_2}\}$,$\{\overline{I_3}\}$, and $\{\overline{I_2},\overline{I_3}\}^*$ emerge from $\{\overline{I_1}\}$ at $w_0=\gamma^{-1}$. In the limit $\gamma\to1$, we have the additional connection with the solution $\{\overline{I_1},\overline{I_2},\overline{I_3}\}$ at $w_0=1$, with the solution $\{\overline{I_1},\overline{I_2},\overline{I_3}\}^*$ at $w_0=w_1=w_2=1$, and with the solution $\{\overline{I_1},\overline{I_2},\overline{I_3}\}^{**}$ at $w_0=w_2=1$.

B. Monomode solutions $\{\overline{I_k}\}$

1. Solution $\{\overline{I_1}\}$

This solution is

$$\overline{I_1}=2\frac{\overline{D_0}-1}{2-\overline{D_0}},\quad \overline{I_2}=\overline{I_3}=0,$$

$$\overline{N_1}=\overline{D_0}-1,\quad \overline{N_2}=\overline{N_3}=\overline{D_1}\frac{\overline{D_0}-1}{\overline{D_0}},$$

$$w_0=\frac{-\overline{D_0}^2+4\overline{D_0}-2}{2-\overline{D_0}},\quad w_1=w_0\frac{\overline{D_1}}{\overline{D_0}},\quad w_2=\frac{\overline{D_0}\,\overline{D_2}}{2-\overline{D_0}}.$$

The positivity of $\overline{I_1}$ requires $1<\overline{D_0}<2$. This constraint determines $\overline{D_0}$ as a function of w_0 in a unique way when the system is in state $\{\overline{I_1}\}$. A linear stability analysis of this solution yields a double real root whose real part may change sign

$$\lambda_1=-k[\gamma\overline{D}_1(\overline{D}_0-1)-\overline{D}_0(\gamma\overline{D}_0-1)]\overline{D}_0^{-1}.$$

The resulting stability condition is

$$\overline{D}_1>\overline{D}_0(\overline{D}_0-\gamma^{-1})/(\overline{D}_0-1). \tag{21}$$

When long-wavelength population gratings are suppressed ($w_i=\overline{D}_i=0,\ i=2,3$), this inequality reduces to $\overline{D}_0<\gamma^{-1}$, a familiar result in the TSD theory. On the contrary, if w_1 is varied in order to meet Eq. (21) the laser can be forced to remain monomode even with $\gamma^{-1}<\overline{D}_0$, i.e., beyond the multimode threshold with regard to the average pumping predicted via the TSD analysis.

There is also one pair of complex roots

$$\lambda_{2,\pm}=\frac{6-12\overline{D}_0+3\overline{D}_0^2}{16-12\overline{D}_0+2\overline{D}_0^2}\pm i\sqrt{k(w_0-1)}.$$

The imaginary part of these roots is the relaxation oscillation frequency Ω_R of the single-mode laser. This root does not lead to an instability. The remaining roots are real and negative.

At the bifurcation point $\lambda_1=0$, the solution $\{\overline{I}_1\}$ is connected to the branches of solutions $\{\overline{I}_1,\overline{I}_2\}$ and $\{\overline{I}_1,\overline{I}_2,\overline{I}_3\}$. The condition $\lambda_1=0$ defines a surface in the pump parameter space $\{w_1,w_2,w_3\}$. In addition, if $\gamma=1$, we can add that $\{\overline{I}_1\}$ is connected at the bifurcation point $\lambda_1=0$ to the solution $\{\overline{I}_1,\overline{I}_2,\overline{I}_3\}^*$ along the line $\overline{D}_0=\overline{D}_1=\overline{D}_2$ and to the solution $\{\overline{I}_1,\overline{I}_2,\overline{I}_3\}^{**}$ along the line $\overline{D}_0=\overline{D}_1=1$.

2. Solution $\{\overline{I}_2\}$

This solution is

$$\overline{I}_1=\overline{I}_3=0,\ \overline{I}_2=2\frac{\overline{D}_0-\gamma^{-1}}{2-\gamma\overline{D}_0},$$

$$\overline{N}_1=\overline{D}_1\frac{\overline{D}_0-\gamma^{-1}}{\overline{D}_0},\ \overline{N}_2=\overline{D}_0-\gamma^{-1},\quad \overline{N}_3=\overline{D}_2\frac{\overline{D}_0-\gamma^{-1}}{\overline{D}_0},$$

$$w_0=\frac{-\gamma\overline{D}_0^2+4\overline{D}_0-2\gamma^{-1}}{2-\gamma\overline{D}_0},$$

$$w_1=\overline{D}_1\frac{2\overline{D}_0-\gamma^{-1}}{\overline{D}_0(2-\gamma\overline{D}_0)},\ w_2=w_1\frac{\overline{D}_2}{\overline{D}_1}.$$

The solution $\{\overline{I}_3\}$ is obtained by permuting $(\overline{I}_2,\overline{N}_2)$ and $(\overline{I}_3,\overline{N}_3)$.

The condition of existence of this solution, $\overline{I}_2>0$, leads to $\gamma^{-1}<\overline{D}_0<2\gamma^{-1}$. A linear stability analysis of the $\{\overline{I}_2\}$ solution yields two real roots that may vanish, a pair of complex conjugate roots with negative real parts, and five real roots that are negative. The two critical real roots are

$$\lambda_1=-k[\overline{D}_1(\overline{D}_0-\gamma^{-1})-\overline{D}_0(\overline{D}_0-1)]\overline{D}_0^{-1},$$

which is negative if

$$\overline{D}_1>\overline{D}_0\frac{\overline{D}_0-1}{\overline{D}_0-\gamma^{-1}}, \tag{22}$$

and the root

$$\lambda_2=-k(\gamma\overline{D}_0-1)(\overline{D}_2-\overline{D}_0)\overline{D}_0^{-1}, \tag{23}$$

which is negative if $\overline{D}_2>\overline{D}_0$. If $\lambda_1<0$ and $\lambda_2<0$, a stable monomode oscillation can thus be achieved with a mode whose gain is smaller than the gain of the other modes. However, the domains of stability of solutions $\{\overline{I}_1\}$ and $\{\overline{I}_2\}$ (or $\{\overline{I}_3\}$) overlap in the pump parameter space $\{w_0,w_1,w_2\}$, as discussed in Sec. IV F.

At the bifurcation point $\lambda_1=0$, the solution $\{\overline{I}_2\}$ becomes unstable and the solution $\{\overline{I}_1,\overline{I}_2\}$ emerges. At the boundary $\lambda_2=0$, the solution $\{\overline{I}_2\}$ becomes unstable and the solution $\{\overline{I}_2,\overline{I}_3\}^*$ emerges. In addition, we can show for $\gamma=1$ that the solution $\{\overline{I}_2\}$ is connected to the solution $\{\overline{I}_1,\overline{I}_2,\overline{I}_3\}^*$ along the line $\overline{D}_0=\overline{D}_1=\overline{D}_2$.

The characteristic polynomial of the linearized system has also two complex conjugate roots with negative real part

$$\lambda_\pm=-\frac{6-12\gamma\overline{D}_0+3\gamma^2\overline{D}_0}{-16+12\gamma\overline{D}_0-2\gamma^2\overline{D}_0}\pm i\sqrt{k\frac{(4-\gamma\overline{D}_0)(\gamma\overline{D}_0-1)}{2-\gamma\overline{D}_0}}.$$

The imaginary part is different from the McCumber frequency, though it reduces to Ω_R for $\gamma\to1$.

C. Two-mode solutions

1. Solution $\{\overline{I}_1,\overline{I}_2\}$

This solution is

$$\overline{I}_1=2\frac{\overline{D}_1(\overline{D}_0-\gamma^{-1})-\overline{D}_0(\overline{D}_0-1)}{(\overline{D}_1-\overline{D}_0)[\overline{D}_1-3\overline{D}_0+2(1+\gamma^{-1})]},$$

$$\overline{I}_2=2\frac{\overline{D}_1(\overline{D}_0-1)-\overline{D}_0(\overline{D}_0-\gamma^{-1})}{\gamma(\overline{D}_1-\overline{D}_0)[\overline{D}_1-3\overline{D}_0+2(1+\gamma^{-1})]},$$

$$\overline{I}_3=0,\quad N_1=\overline{D}_0-1,\quad N_2=\overline{D}_0-\gamma^{-1},$$

$$N_3=\{\overline{D}_1[\overline{D}_1(\overline{D}_0-\gamma^{-1})-\overline{D}_0(\overline{D}_0-1)]+\overline{D}_2[\overline{D}_1(\overline{D}_0-1)-\overline{D}_0(\overline{D}_0-\gamma^{-1})]\}[\overline{D}_1^2-\overline{D}_0^2]^{-1},$$

$$w_0=\overline{D}_0+\overline{I}_1+\overline{I}_2,$$

$$w_1=(1+\gamma\overline{I}_2+\overline{I}_1)\overline{D}_1-\frac{1}{2}[\gamma\overline{I}_2N_1+\overline{I}_1(N_2+N_3)],$$

$$w_2=(1+\gamma\overline{I}_2+\overline{I}_1)\overline{D}_2-\frac{1}{2}\gamma\overline{I}_2N_3. \tag{24}$$

The positivity of the modal intensities I_1 and I_2 yields the condition

$$(\overline{D}_0-1)(4-3\overline{D}_0+\overline{D}_1)>0.$$

Using Eq. (20), one easily finds a first root of the characteristic polynomial $\lambda_1=k[-1+\gamma(\overline{D}_0-N_3)]$. The stability condition $\lambda_1<0$ yields

$$[\gamma\overline{D}_1(\overline{D}_0-1)(\overline{D}_2-\overline{D}_0)+(\gamma\overline{D}_0-1)(\overline{D}_1^2-\overline{D}_0\overline{D}_2)]\times(\overline{D}_1^2-\overline{D}_0^2)^{-1}>(\gamma\overline{D}_0-1). \quad (25)$$

At this instability point, the two-mode solution is connected to the three-mode solution $\{\overline{I}_1,\overline{I}_2,\overline{I}_3\}$**. In the limit $\gamma\to1$, this stability condition reduces to $\overline{D}_2>\overline{D}_0$. Further investigation of the characteristic polynomial was carried out in the limit $\gamma\to1$. Taking advantage of the fact that $k\gg1$, we found an approximate expression for two pairs of complex conjugate roots, the first of which is

$$\lambda_{2,\pm}=-\frac{\overline{D}_0+\overline{D}_1}{2(4-3\overline{D}_0+\overline{D}_1)}\pm\lim_{\gamma\to1}\sqrt{k\overline{I}_2(\overline{D}_0-\overline{D}_1)/2}+O(k^{-1/2}).$$

They are stable provided that $\overline{D}_0>\overline{D}_1$; otherwise $\lambda_{2,+}$ is real and positive. The second pair of complex conjugate roots have their imaginary part equal to the McCumber frequency

$$\lambda_{3,\pm}=a\pm i\Omega,\quad \Omega=\Omega_R+O(k^{-1/2}),$$

$$a=-\frac{w_1+5w_0}{2(8-3\overline{D}_0+\overline{D}_1)}+O(k^{-1}). \quad (26)$$

The real part of this pair of roots is positive for $w_1+5w_0<0$. In that case, the system undergoes a Hopf bifurcation. In Sec. IV E, we shall present an analysis of the periodic solutions suggesting that this bifurcation is subcritical. Numerically, a periodic pulsed solution has been found for $w_0=1.1$, $w_1=-5.51$, and $w_2=2$. The value of w_2 is suggested by the condition $\overline{D}_2>\overline{D}_0$. Decreasing w_1, we observed a period-doubling cascade, chaos, and chaotic passive Q-switching (PQS). Period-two $\overline{I}_1$ pulses antiphased with period-two $\overline{I}_2$ pulses thus leading to period-one pulsing for the total intensity.

2. Solution $\{\overline{I}_2,\overline{I}_3\}$

This solution is

$$\overline{I}_1=0,\ \overline{I}_2=\overline{I}_3=2\frac{\overline{D}_0-\gamma^{-1}}{4-3\gamma\overline{D}_0+\gamma\overline{D}_2},$$

$$\overline{N}_1=2\overline{D}_1\frac{\overline{D}_0-\gamma^{-1}}{\overline{D}_0+\overline{D}_2},\ \overline{N}_2=\overline{N}_3=\overline{D}_0-\gamma^{-1},$$

$$w_0=\frac{8\overline{D}_0-3\gamma\overline{D}_0^2+\gamma\overline{D}_2\overline{D}_0-4\gamma^{-1}}{4-3\gamma\overline{D}_0+\gamma\overline{D}_2},$$

$$w_1=\frac{\overline{D}_1(2-\gamma\overline{D}_0+\gamma\overline{D}_2)(-2+3\gamma\overline{D}_0+\gamma\overline{D}_2)}{\gamma(\overline{D}_0+\overline{D}_2)(4-3\gamma\overline{D}_0+\gamma\overline{D}_2)},$$

$$w_2=\frac{\gamma\overline{D}_2^2-2\gamma\overline{D}_0^2+\gamma\overline{D}_0\overline{D}_2+4\overline{D}_0-2\gamma^{-1}}{4-3\gamma\overline{D}_0+\gamma\overline{D}_2}.$$

The positivity of the intensities requires

$$(\overline{D}_0-\gamma^{-1})(4-3\gamma\overline{D}_0+\gamma\overline{D}_2)>0. \quad (27)$$

A real root of the characteristic equation is $\lambda_1=k(-1+\overline{D}_0-\overline{N}_1)$. Stability requires

$$2\overline{D}_1>(\overline{D}_0+\overline{D}_2)\frac{\overline{D}_0-1}{\overline{D}_0-\gamma^{-1}}, \quad (28)$$

which implies a depletion of the inversion profile at the center of the cavity and therefore a competition between mode 1 and modes 2 and 3. If this condition is not fulfilled, a transition to the solution $\{\overline{I}_1,\overline{I}_2,\overline{I}_3\}$ takes place. The other stability conditions were obtained in the limit $\gamma\to1$. Two real roots of the characteristic polynomial are

$$\lambda_2=-\frac{2-\overline{D}_0+\overline{D}_2}{4-3\overline{D}_0+\overline{D}_2},\ \lambda_3=-\frac{-2+3\overline{D}_0+\overline{D}_2}{4-3\overline{D}_0+\overline{D}_2}. \quad (29)$$

Two pairs of complex conjugate roots have been found in the double limit $\gamma\to1$ and $k\gg1$. The first pair is

$$\lambda_{4,\pm}=-\frac{\overline{D}_0+\overline{D}_2}{2(4-3\overline{D}_0+\overline{D}_2)}\pm i\lim_{\gamma\to1}\sqrt{k\overline{I}_2(\overline{D}_0-\overline{D}_2)/2}, \quad (30)$$

whose imaginary part is different from the McCumber frequency and exist only if $\overline{D}_0>\overline{D}_2$. The roots $\lambda_{4,\pm}$, λ_2, and λ_3 are stable provided the condition (27) is fulfilled. If $\overline{D}_0=\overline{D}_2$, the solution $\{\overline{I}_2,\overline{I}_3\}$ is connected to the solution $\{\overline{I}_2,\overline{I}_3\}$*. There is also a pair of complex conjugate roots associated with the McCumber frequency

$$\lambda_{5,\pm}=a\pm i\Omega,\quad \Omega=\Omega_R,\quad a=-\frac{w_2+5w_0}{2(8-3\overline{D}_0+\overline{D}_2)}. \quad (31)$$

A Hopf bifurcation occurs at $w_2+5w_0=0$ which will be studied in Sec. IV E. Numerically, we have observed in-phase period-two pulsed solutions, antiphase period-two pulsed solutions, chaos, regular antiphase pulses, and chaotic PQS, respectively, by decreasing w_2 from -5.5 to -6.2 with $w_0=1.1$ and $w_1=0$.

3. Solution $\{\overline{I_2},\overline{I_3}\}^*$

This family of solutions is given by

$$\overline{I_2}+\overline{I_3}=2\frac{\overline{D_0}-\gamma^{-1}}{2-\gamma\overline{D_0}},\quad N_1=\overline{D_1}\frac{\overline{D_0}-\gamma^{-1}}{\overline{D_0}},$$

$$\overline{I_1}=0,\quad \overline{D_0}=\overline{D_2},\quad \overline{N_2}=\overline{N_3}=\gamma^{-1},$$

$$w_0=\frac{-2\gamma^{-1}+4\overline{D_0}-\gamma\overline{D_0^2}}{2-\gamma\overline{D_0}},\quad w_1=\frac{\overline{D_1}(2\overline{D_0}-\gamma^{-1})}{\overline{D_0}(2-\gamma\overline{D_0})},$$

$$w_2=\frac{2\overline{D_0}-\gamma^{-1}}{\overline{D_0}(2-\gamma\overline{D_0})}.$$

The peculiar property of this family of solutions is that the lasing modal intensities are not fixed: Only the total intensity is determined. The value of the modal intensities $\overline{I_2}$ and $\overline{I_3}$ depends on the initial conditions. This branch of solutions connects the solution $\{\overline{I_2}\}$ at $\lambda_2=0$, where λ_2 is given by Eq. (23) to the solution $\{\overline{I_2},\overline{I_3}\}$. We recall that no stability analysis is presented for the $\{\}^*$ and $\{\}^{**}$ solutions since they are of measure zero.

D. Three-mode solutions

The symmetric three-mode TSD^+ model has three different steady-state solutions with all modes above the lasing threshold. In this section we only define analytically these solutions and recall which steady solutions they connect. In Sec. IV E, we shall derive a general expression for the Hopf bifurcation which is another source of instability.

1. Solution $\{\overline{I_1},\overline{I_2},\overline{I_3}\}$

This solution is given by

$$\overline{N_1}=\overline{D_0}-1,\quad \overline{N_2}=\overline{N_3}=\overline{N}=\overline{D_0}-\gamma^{-1},$$

$$\overline{I_1}=[2\overline{ND_1}-\overline{N_1}(\overline{D_0}+\overline{D_2})]M^{-1},$$

$$\overline{I_2}=\overline{I_3}=[\overline{N_1}\overline{D_1}-\overline{ND_0}](\gamma M)^{-1},$$

$$w_0=\overline{D_0}+\overline{I_1}+\overline{I_2}+\overline{I_3},$$

$$w_1=(1+\gamma\overline{I_2}+\overline{I_1}+\gamma\overline{I_3})\overline{D_1}-\frac{1}{2}[\gamma\overline{I_2}\overline{N_1}+\overline{I_1}(\overline{N_2}+\overline{N_3})+\gamma\overline{I_3}\overline{N_1}],$$

$$w_2=(1+\gamma\overline{I_2}+\overline{I_1}+\gamma\overline{I_3})\overline{D_2}-\frac{1}{2}(\gamma\overline{I_2}\overline{N_3}+\gamma\overline{I_3}\overline{N_2}).$$

where

$$M=\overline{D_1}[\overline{D_1}-2(\overline{N}+\overline{N_1})]+\overline{D_0}[2\overline{N}+\overline{N_1}-(\overline{D_0}+\overline{D_2})/2]+\overline{D_2}\overline{N_1}.$$

The characteristic polynomial that rules the linear stability of this solution factorizes into second- and seventh-order polynomials in the limit $\gamma\to1$. The roots of the quadratic are

$$\lambda_\pm=\frac{1}{2}\{-(1+\overline{I_1}+2\overline{I_2})\pm\sqrt{(1+\overline{I_1}+2\overline{I_2})^2-2k\overline{I_2}(\overline{D_0}-\overline{D_2})}\}.\qquad(32)$$

Since $k\gg1$, these roots are complex conjugate with a negative real part if $\overline{D_0}>\overline{D_2}$. The imaginary part is $\omega=\sqrt{k\overline{I_2}(\overline{D_0}-\overline{D_2})/2}+O(k^{-1/2})$. Otherwise, they are real and λ_+ is positive. Of course, this instability is linked to the competition between modes 2 and 3, as can be seen from Table I. If $\overline{D_2}>\overline{D_0}$, either 2 or 3 can be above threshold.

2. Solutions $\{\overline{I_1},\overline{I_2},\overline{I_3}\}^*$

This family of solutions is characterized by $\overline{I_2}\neq\overline{I_3}$ and $\overline{I_1}\neq\overline{I_2}+\overline{I_3}$, which implies that $\overline{D_0}=\overline{D_1}=\overline{D_2}$. In the limit $\gamma\to1$, we have

$$\overline{I_1}+\overline{I_2}+\overline{I_3}=2\frac{\overline{D_0}-1}{2-\overline{D_0}},$$

$$\overline{N_1}=\overline{N_2}=\overline{N_3}=\overline{D_0}-1,$$

$$w_0=\frac{-2+4\overline{D_0}-\overline{D_0^2}}{2-\overline{D_0}},\quad w_1=\frac{2\overline{D_0}-1}{2-\overline{D_0}}-\frac{\overline{D_0}-1}{2}\overline{I_1},$$

$$w_2=\frac{\overline{D_0^2}}{2-\overline{D_0}}-\frac{\overline{D_0}-1}{2}(\overline{I_2}+\overline{I_3}).$$

3. Solutions $\{\overline{I_1},\overline{I_2},\overline{I_3}\}^{**}$

This family of solutions is considered only in the limit $\gamma\to1$, where it is characterized by $\overline{I_2}\neq\overline{I_3}$ but $\overline{I_1}=\overline{I_2}+\overline{I_3}$:

$$\overline{I_1}=2\frac{\overline{D_0}-1}{4-3\overline{D_0}+\overline{D_1}},\quad \overline{I_1}=\overline{I_2}+\overline{I_3},$$

$$\overline{D_0}=\overline{D_2},\quad \overline{N_1}=\overline{N_2}=\overline{N_3}=\overline{D_0}-1,$$

$$w_0=\frac{-4+8\overline{D_0}+\overline{D_0}\overline{D_1}-3\overline{D_0^2}}{4-3\overline{D_0}+\overline{D_1}},\quad w_2=\frac{-1+2\overline{D_0}+\overline{D_0}\overline{D_1}}{4-3\overline{D_0}+\overline{D_1}},$$

$$w_1=\frac{-3+6\overline{D_0}+\overline{D_0}\overline{D_1}-3\overline{D_0^2}+\overline{D_1^2}}{4-3\overline{D_0}+\overline{D_1}}.$$

This family of solutions connects the branches $\{\overline{I_1},\overline{I_2}\}$ and $\{\overline{I_1},\overline{I_2},\overline{I_3}\}$.

E. Pulsed solutions

We have shown in the previous sections that there are Hopf bifurcations to self-pulsing states. We have been able to derive a general expression for the Hopf bifurcation points only for two-mode solutions and in the limit $\gamma\to1$. The sta-

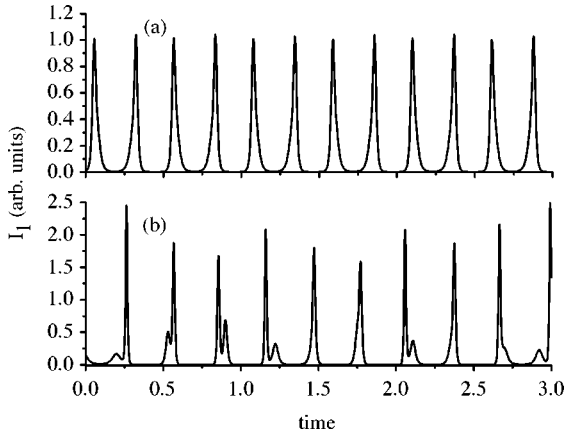

FIG. 1. (a) Periodic solution emerging from the steady-state solution $\{I_1, I_2\}$ for $w_0 = 1.1$, $w_1 = -5.56$, and $w_2 = 2$. (b) Chaotic solution for $w_0 = 1.1$, $w_1 = -5.82$, and $w_2 = 2$.

bility of the emerging periodic solutions has not been determined. We shall therefore use an indirect method to derive more information on the self-pulsing solutions. It is based on the fact that the solutions observed numerically are pulsed (see Fig. 1), which means that for each mode, intensity peaks are separated by domains of vanishingly small intensity. Thus these solutions represent a trajectory, in phase space, between the unstable $\{\varnothing\}$ solution and some unstable finite-intensity solution. The pulsing character of these solutions has the following origin. The first lasing threshold is $\bar{D}_0 = 1$, which means that only the average population inversion affects the switching on of the laser. However, one can maintain $\bar{D}_0 < 1$ while storing energy in the material medium by having w_1 and/or w_2 strongly negative. As shown in Table I, this is possible by pumping selectively at $z = nL/4$ with $n = 1$, 2, or 3. If there is enough energy stored in this way, bringing the average population inversion above the first lasing threshold induces a cycle as in PQS: The energy stored by way of population inversion is released in the field, which builds up abruptly. This depletes the population inversion and soon again the average population inversion is below threshold. To use this information, we seek interpulse solutions of the form

$$I_k = \varepsilon i_k + O(\varepsilon^2), \quad D_k = w_k + \varepsilon d_k + O(\varepsilon^2),$$

$$N_k = \varepsilon n_k + O(\varepsilon^2), \tag{33}$$

where $\varepsilon = 1/k$. To leading order in ε this yields

$$\frac{di_1}{dt} = i_1(\bar{w}_1 + d_0 - n_1),$$

$$\frac{di_2}{dt} = i_2(\bar{w}_2 + \gamma d_0 - \gamma n_2),$$

$$\frac{di_3}{dt} = i_3(\bar{w}_2 + \gamma d_0 - \gamma n_3),$$

$$\frac{dd_k}{dt} = -d_k - (\gamma i_2 + i_1 + \gamma i_3) w_k,$$

$$\frac{dn_1}{dt} = -n_1 + \frac{1}{2}(\gamma i_2 w_1 + i_1 w_0 + \gamma i_3 w_1),$$

$$\frac{dn_2}{dt} = -n_2 + \frac{1}{2}(\gamma i_2 w_0 + i_1 w_1 + \gamma i_3 w_2),$$

$$\frac{dn_3}{dt} = -n_3 + \frac{1}{2}(\gamma i_2 w_2 + i_1 w_1 + \gamma i_3 w_0),$$

where we have introduced the expansions $\bar{w}_1 = k(w_0 - 1) + O(1/k)$ and $\bar{w}_2 = k(\gamma w_0 - 1) + O(1/k)$ to have a correct balance in the intensity equations. Note that the time has not been scaled. Since there is no Hopf bifurcation in the single-mode solutions, we directly consider the two-mode solutions.

1. Two-mode solutions

Let us first study the solution $\{I_1, I_2\}$. Introducing the auxiliary variables $x_k = \ln(i_k)$, it is easy to derive

$$x_1'' + x_1' = \bar{w}_1 - B_0 e^{x_1} - \gamma B_1 e^{x_2},$$

$$x_2'' + x_2' = \bar{w}_2 - \gamma B_1 e^{x_1} - \gamma^2 B_0 e^{x_2},$$

where $x' \equiv dx/dt$ and $B_q = w_0 + w_q/2$. It can be shown that the solutions x_k may diverge in a finite time, depending on the B_q. Therefore, we seek solutions of the form $x_k = c_{k1} + c_{k2}\ln(|t-a|) + c_{k3}(t-a)$. In this expression, a is an integration constant, which is determined by matching considerations with the pulsed part of the solution. Since we do not attempt to describe the pulse, we leave this constant undetermined in the remainder of our discussion. This leads to $c_{12} = c_{22} = -2$, $c_{13} = \bar{w}_1$, $c_{23} = \bar{w}_2$, and an algebraic system for the $\{c_{k1}\}$ whose solutions is

$$e^{c_{11}} = \frac{2}{\gamma}\frac{B_1 - \gamma B_0}{B_0^2 - B_1^2}, \quad e^{c_{21}} = \frac{2}{\gamma^2}\frac{\gamma B_1 - B_0}{B_0^2 - B_1^2}.$$

Imposing $e^{c_{k1}} > 0$ gives a condition that turns out to be the expression for the Hopf bifurcation point. In the limit $\gamma = 1$, the existence of the solution $\{c_{k1}\}$ requires $B_0 + B_1 < 0$ or equivalently $5w_0 < -w_1$, which is the result (26) we have derived in the conventional way. For arbitrary γ, there are two sets of three conditions: $B_0^2 \gtrless B_1^2$, $B_1 \gtrless \gamma B_0$, and $\gamma B_1 \gtrless B_0$. Analyzing these conditions, it is easy to prove that it is the lower inequality sign that must be retained and it reduces to $5w_0 < -w_1$. This proves that the Hopf bifurcation threshold is independent of γ.

We have constructed in this way, in the self-pulsing domain, a solution of small amplitude, being of order ε, which is expected to connect two consecutive pulses. The presence of the pulse is attested by the divergence. This is not a solution that emerges from the Hopf bifurcation since close to the bifurcation point the solution is harmonic in time. Hence the piece of solution we have just constructed belongs to an upper branch, which suggests that the Hopf bifurcation is subcritical. This conjecture is supported by numerical simulations.

A similar result is obtained for the two-mode solution $\{I_2, I_3\}$. We obtain for the coefficients $\{c_{k1}\}$ the expression

$$e^{c_{21}}=e^{c_{31}}=\frac{-2}{\gamma^2(B_0+B_2)}.$$

The condition of existence of these solutions is $B_0+B_2<0$, i.e., $5w_0+w_2<0$, which is also independent of γ. This is the threshold condition (31) derived in the usual way, though for $\gamma\to 1$ only, in Sec. IV C. Here again a subcritical Hopf bifurcation induces a transition directly from the steady states to the PQS regime.

2. Multimode solution

The method used to construct the interpulse solutions is readily generalized to an arbitrary number of modes and an arbitrary distribution of linear gains γ_q. The linear equations for the $\{\exp c_{k1}\}$ are

$$\sum_{q'\in\mathcal{Q}}\gamma_{q'}e^{c_{q'1}}B(q-q')=-2/\gamma_q,\quad q\in\mathcal{Q}.$$

For the three-mode regime, the coefficients c_{k1} are given by

$$e^{c_{11}}=\frac{2}{\gamma}\,\frac{2B_2-\gamma(B_1+B_3)}{B_1(B_1+B_3)-2B_2^2},$$

$$e^{c_{21}}=e^{c_{31}}=\frac{2}{\gamma^2}\,\frac{\gamma B_2-B_1}{B_1(B_1+B_3)-2B_2^2}.$$

The threshold conditions are somewhat more complex to study. Analyzing the expressions for the $\{c_{k1}\}$ yields that the periodic solutions exist in the domain defined by $B_1(B_1+B_3)<2B_2^2$ and $2B_2<\gamma(B_1+B_3)$. The locus of the Hopf bifurcations is a section of the curve $B_1(B_1+B_3)=2B_2^2$, which can also be expressed as $w_2=2w_1^2/3w_0+8w_1/3-7w_0/3$. In the plane (w_2,w_1), this locus is bounded by the intersection with the line $2B_2=\gamma(B_1+B_3)$, which takes place at $(w_2,w_1)=(-5w_0,-2w_0)$, and by the point, where $\overline{D}_0=\overline{D}_2$, since from there on the solution $\{\overline{I}_1,\overline{I}_2,\overline{I}_3\}$ bifurcates to the solution $\{\overline{I}_2,\overline{I}_3\}$. Here again the Hopf bifurcation is expected to be subcritical, in full agreement with the numerical simulations.

F. Hysteresis

Another difference between the TSD and the TSD$^+$ equations is the occurrence of hysteresis domains for the steady-state solutions. The analytic expression of the single-mode solutions $\{\overline{I}_k\}$ in terms of the $\{w_k\}$ is too complex to be of much use for a general discussion of the hysteresis domains. Therefore, we shall illustrate this effect by a simple example. We consider a closed loop in the (w_1,w_2) plane with $w_0=1.75$ and $\gamma=0.9$. The result is displayed in Fig. 2 and shows that starting with the $\{\overline{I}_1\}$ solution, we end up at the same point in parameter space, but with the $\{\overline{I}_2\}$ solution. The initial and final states are connected, successively, by the states $\{\overline{I}_1,\overline{I}_2\}$, $\{\overline{I}_1,\overline{I}_2,\overline{I}_3\}$, and $\{\overline{I}_2,\overline{I}_3\}$. Only one of the two parameters w_1 and w_2 is changed at a time.

The first step is to weaken competition between I_1 and I_2 by decreasing w_1. The system bifurcates from $\{\overline{I}_1\}$ to $\{\overline{I}_1,\overline{I}_2\}$ when λ_1 given by Eq. (21) vanishes, that is, at $(w_1,w_2)=(0.94,2)$. Second, mode 3 is forced to oscillate by decreasing w_1 to zero and then decreasing w_2. A bifurcation $\{\overline{I}_1,\overline{I}_2\}\to\{\overline{I}_1,\overline{I}_2,\overline{I}_3\}$ occurs at $(w_1,w_2)=(0,1.82)$ as a consequence of Eq. (25). The parameter w_2 is decreased further in order to extinguish mode 1, as expected from the stability condition (32). Indeed, at $(w_1,w_2)=(0,-3.5)$, the system bifurcates from $\{\overline{I}_1,\overline{I}_2,\overline{I}_3\}$ to $\{\overline{I}_2,\overline{I}_3\}$. The next step is to increase w_1 up to 3. This has the effect of strengthening the mode competition between I_1 and I_2. As I_2 is already amplified, I_1 is quenched. Finally, w_2 is increased from -3.5 to 2. At the point (3,1.82), the system undergoes a bifurcation from $\{\overline{I}_2,\overline{I}_3\}$ to either $\{\overline{I}_2\}$ or $\{\overline{I}_3\}$, which follows from condition (30). The final state $\{\overline{I}_2\}$ or $\{\overline{I}_3\}$ depends on fluctuations.

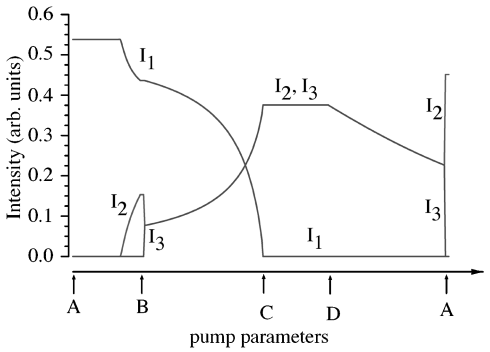

FIG. 2. Modal intensities as a function of w_1 and w_2 for $w_0=1.75$ and $\gamma=0.9$. *A*, $w_1=3$ and $w_2=2$; *B*, $w_1=0$ and $w_2=2$; *C*, $w_1=0$ and $w_2=-3.5$; and *D*, $w_1=3$ and $w_2=-3.5$.

V. CONCLUSION

The results presented in this paper may seem to contradict a little-known theorem on the global stability of the general rate equations expressed as

$$\frac{dI(p,t)}{dt}=\kappa\left(-1+A_p\int_0^L|\phi(p,z)|^2D(z,t)dz\right)I(p,t),\tag{34}$$

$$\frac{dD}{dt}=-\gamma[D(z,t)-D_0(z)]-\beta D(z,t)\times\sum_p\gamma_p|\phi(p,z)|^2I(p,t),\tag{35}$$

from which the TSD and the TSD$^+$ equations are derived as modal expansions. A detailed derivation of the rate equations (34) and (35) is found, for instance, in [12]. The global stability theorem of Antsiferov *et al.* [13] proves that the function

$$\mathcal{L}(t)=\int_0^L\frac{[D(z,t)-\overline{D}(z)]^2}{2\overline{D}(z)}dz+\kappa^{-1}\sum_p\left[I_p(t)-\overline{I}_p-\overline{I}_p\ln\frac{I_p(t)}{\overline{I}_p}\right]$$

is a Lyapunov function since $d\mathcal{L}/dt<0$. The existence of such a function implies that the only dynamics that can take place is a monotonic evolution towards a single steady-state. However, a careful analysis of the proof indicates that it is restricted by the condition $\overline{D}(z)\neq 0$. In other terms, this theorem states that if the steady-state population inversion vanishes nowhere in the domain $0\leqslant z\leqslant L$, there is a unique steady state associated with any initial condition through a momentous evolution. Our results do not contradict this theorem since all the bifurcation conditions obtained in this paper impose constraints on the pump that lead to domains without population inversion and therefore points in space where the population inversion changes sign.

The main point of this paper is that the longitudinal inhomogeneity of the pumping process is the source of new steady states and Hopf bifurcations. The Hopf bifurcations lead to more complex time-dependent solutions, including chaotic solutions. The coincidence of the Hopf bifurcation threshold and the PQS pulsing is surprising since they obviously do not correspond to the same mechanism. The two phenomena occur for the same values of the parameters but on different branches of the same periodic solution. A similar situation has been described for a laser with a saturable absorber [14], though without any more mathematical understanding.

Another consequence of the inhomogeneous longitudinal pumping is the occurrence of solutions such as $\{I_2\}$, $\{I_3\}$, or $\{I_2,I_3\}$, which involve only modes with a lower gain while the mode with the highest gain is off. This is confirmed qualitatively by the results of Gusev *et al.* [15]. In their experiment, a 5-cm-long Nd:YAG crystal (where YAG denotes yttrium aluminum garnet) was translated along the axis of a 80-cm-long cavity. This achieved a highly inhomogeneous pumping profile. Mode locking was observed when the crystal was at $L/2$, the center of the cavity (strongly negative w_1), and also when located at $L/4$ (strongly negative w_2). Spectral analysis revealed that mode spacing was $c/2L$ in the former case and c/L in the latter, in agreement with our theoretical analysis.

ACKNOWLEDGMENTS

This research was supported by the Fonds National de la Recherche Scientifique and the Interuniversity Attraction Pole program of the Belgian government.

[1] C. L. Tang, H. Statz, and G. de Mars, J. Appl. Phys. **34**, 2289 (1963).
[2] J. A. Fleck, Jr. and R. E. Kidder, J. Appl. Phys. **35**, 2825 (1964).
[3] L. A. Ostroskiĭ, Sov. Phys. JETP **21**, 727 (1965).
[4] L. A. Ostroskiĭ, Sov. Phys. JETP **22**, 1053 (1966).
[5] N. G. Basov, V. N. Morozov, and A. N. Oraevskiĭ, Sov. Phys. JETP **22**, 622 (1966).
[6] C. Etrich, P. Mandel, N. B. Abraham, and H. Zeghlache, IEEE J. Quantum Electron. **28**, 811 (1992).
[7] I. V. Koryukin, P. A. Khandokhin, Ya. I. Khanin, and P. Mandel, Kvant. Elektron. (Moscow) **22**, 1081 (1995) [Quantum Electron. **25**, 1045 (1995)].
[8] P. Mandel, C. Etrich, and K. Otsuka, IEEE J. Quantum Electron. **29**, 836 (1993).
[9] D. Pieroux and P. Mandel, Quantum Semiclassic. Opt. **9**, L17 (1997).
[10] D. Pieroux and P. Mandel, Opt. Commun. **107**, 245 (1994).
[11] B. A. Nguyen and P. Mandel, Phys. Rev. E **57**, 1444 (1998).
[12] P. Mandel, *Theoretical Problems in Cavity Nonlinear Optics* (Cambridge University Press, Cambridge, 1997).
[13] V. V. Antsiferov, A. V. Ghiner, K. P. Komarov, and K. G. Folin, Kvant. Elektron. (Moscow) **2**, 591 (1975) [Sov. J. Quantum Electron. **5**, 332 (1976)].
[14] J. C. Antoranz, J. Gea, and M. G. Velarde, Phys. Rev. Lett. **47**, 1895 (1981).
[15] A. A. Gusev, S. V. Kruzhalov, L. N. Pakhomov, and V. Yu. Petrun'kin, Sov. Tech. Phys. Lett. **4**, 503 (1978).